JOURNAL OF MORPHOLOGY 277:948–956 (2016)

Trabecular Bone of Precocials at Birth; Are They Prepared to Run for the Wolf(f)?

Ben M.C. Gorissen,[1]* Claudia F. Wolschrijn,[1] Anouk A.M. van Vilsteren,[2] Bert van Rietbergen,[3] and P. René van Weeren[4]

[1]*Department of Pathobiology, Anatomy and Physiology Division, Faculty of Veterinary Medicine, Utrecht University, Utrecht, The Netherlands*
[2]*Department of Animal Sciences, Human and Animal Physiology Division, Wageningen University, Wageningen, The Netherlands*
[3]*Department of Biomedical Engineering, Orthopedic Biomechanics Division, Eindhoven University of Technology, Eindhoven, The Netherlands*
[4]*Department of Equine Sciences, Faculty of Veterinary Medicine, Utrecht University, Utrecht, The Netherlands*

ABSTRACT Bone is a dynamic tissue adapting to loading according to "Wolff's law of bone adaptation." During very early life, however, such a mechanism may not be adequate enough to adapt to the dramatic change in environmental challenges in precocial species. Their neonates are required to stand and walk within hours after birth, in contrast to altricial animals that have much more time to adapt from the intrauterine environment to the outside world. In this study, trabecular bone parameters of the talus and sagittal ridge of the tibia from stillborn but full-term precocials (calves and foals) were analyzed by micro-CT imaging in order to identify possible anticipatory mechanisms to loading. Calculated average bone volume fraction in the Shetland pony (49–74%) was significantly higher compared to Warmblood foals (28–51%). Bovine trabecular bone was characterized by a low average bone volume fraction (22–28%), however, more directional anisotropy was found. It is concluded that anticipatory strategies in skeletal development exist in precocial species, which differ per species and are most likely related to anatomical differences in joint geometry and related loading patterns. The underlying regulatory mechanisms are still unknown, but they may be based on a genetic blueprint for the development of bone. More knowledge, both about a possible blueprint and its regulation, will be helpful in understanding developmental bone and joint diseases. J. Morphol. 277:948–956, 2016.

KEY WORDS: neonate; development; micro-CT; Wolff's law

INTRODUCTION

Loading of bone starts already during intrauterine skeletal development (Pitsillides, 2006; Rot et al., 2014) and continues during growth after birth and in all phases of life thereafter (Yokota et al., 2011; Dowthwaite et al., 2014; Torcasio et al., 2014). According to "Wolff's law of bone adaptation" (Wolff, 1892), which forms the basis for the mechanostat theory, explaining the relationship between loading and bone remodeling (Frost, 2001), bone mass will decrease when loaded below a certain threshold and increase in reaction to loading above this threshold, achieving an optimal form to withstand prevailing forces (Huiskes et al., 1987; Frost, 2001; MacLatchy and Müller, 2002; Christen et al., 2014).

Eutherian mammals differ in the degree of development at birth. Precocials, such as foals and calves, are born relatively mature and are able to stand and walk within hours after birth. On the other hand, altricials, like dogs, produce offspring born in a relatively poor state of development. No sharp division can be made between altricial and precocial, as it is a gradient characteristic. Being precocial has major consequences for the bones of the axial and appendicular skeleton, as skeletal loading changes dramatically after birth. During gestation, limbs are folded and not weight bearing, limiting loading to forces generated by intrauterine muscle contractions. After birth limbs are extended, carry weight and in precocials are subjected to considerable forces generated by locomotion, only hours after leaving the uterine environment.

To withstand these forces, the ossification process has progressed much further in the precocial neonate, compared to altricial species. In new-born puppies,

The copyright line for this article was changed on 8 November 2016 after original online publication.

Additional Supporting Information may be found in the online version of this article.

*Correspondence to: Ben M.C. Gorissen, Department of Pathobiology, Anatomy and Physiology Division, Faculty of Veterinary Medicine, Utrecht University, Yalelaan 1, 3584 CL Utrecht, The Netherlands.
E-mail: b.m.c.gorissen@uu.nl

Received 22 December 2015; Revised 18 February 2016;
Accepted 20 March 2016.

Published online 20 April 2016 in
Wiley Online Library (wileyonlinelibrary.com).
DOI 10.1002/jmor.20548

the ossification process of short bones starts around birth and most epiphyses are still completely cartilaginous (Evans, 1993). Ossification has progressed much further in neonatal foals and calves, with only a small band of growth and articular cartilage still present at their epiphyses and short bones (Küpfer and Schinz, 1923; Nickel et al., 2005; Fontaine et al., 2013).

Most research on trabecular bone structure of neonates has been performed in long bones of altricial species, and it has been reported that bone volume fraction (BV/TV; BV= bone volume, TV= total volume) followed a U-shaped curve after birth. For example, in the human femur and tibia, average BV/TV at birth is about 50% and decreases to values around and sometimes even under 20% between 6 and 12 months of age. After this period, BV/TV increases again, to reach final values, similar to adult, at an age of 6 years (Ryan and Krovitz, 2006; Gosman and Ketcham, 2009). In dogs BV/TV follows a comparable U-shaped curve, with lowest BV/TV values found at about 8 weeks after birth (Wolschrijn and Weijs, 2004). As both in humans and in dogs lowest BV/TV values are reported around the onset of walking, the drop in BV/TV could be explained by mini-modeling, associated with the development of a more preferential orientation of trabeculae, due to the increasing demands of locomotion. During this process, trabeculae that are loaded under a certain threshold disappear and as a result of this, directional anisotropy (DA) increases (Tanck et al., 2001; Wolschrijn and Weijs, 2004).

There is evidence that at least in a number of species, this process begins during gestation. Significant trabecular bone DA was shown at birth in the mule deer and ovine calcaneus (Skedros et al., 2004, 2007). Furthermore, a trabecular architecture fitting with loading during bipedal locomotion has been reported in human neonatal ilia (Cunningham and Black, 2009). The observed DA of the pelvis is not likely to be the result of intrauterine strain-related adaptation, suggesting that at least parts of the skeleton are anticipating future loading, possibly based on a genetic blueprint (Cunningham and Black, 2009).

Bone strength is highly dependent on bone volume (Kabel et al., 1999; Borah et al., 2000; Ryan et al., 2010) and architecture (Ulrich et al., 1997; Mittra et al., 2005). Besides having a further advanced ossification process and hence a higher bone volume, we hypothesized that in neonatal calves and foals trabecular bone microarchitecture already anticipates postnatal loading requirements and thus reflects future rather than past function. Since the Warmblood horse has increased considerably in height at withers over the past 50 years due to selective breeding (Ducro et al., 2009), we also investigated Shetland ponies which have not been subject to strong selection pressure, to exclude possible artificial influences. To verify our hypothesis, microarchitecture of the distal tibia and the talus of stillborn but full-term calves, Shetland pony and Warmblood foals was analyzed and compared by means of micro-CT imaging. More insight into prenatal bone development and its underlying regulatory mechanisms may lead to a better understanding of bone growth and development. It might also provide clues for unraveling pathogenic mechanisms and even for the development of new therapeutic approaches for both developmental (joint) diseases and problems associated with aberrant endochondral ossification later in life, such as osteoarthritis (Staines et al., 2013).

MATERIALS AND METHODS

Animals

Because of ethical considerations no animals were euthanized for this study. Tarsal joints of full-term Holstein-Friesian (HF) calves (*Bos Taurus,* $n = 5$), Dutch Warmblood foals (*Equus ferus caballus,* $n = 5$), and Shetland ponies (*Equus ferus caballus,* $n = 3$) were obtained with owners' consent from (para)clinical departments of the Faculty of Veterinary Medicine, Utrecht University, and from private veterinary practices. To exclude effects of postnatal loading, we collected only material from animals that were either stillborn or euthanized within 12 h after birth. Gestational time and cause of death were recorded, and animals were only included if the cause of death could be considered to have no effect on development. Except for two Dutch Warmblood foals, all animals died because of dystocia, caused by either an abnormal intrauterine position or a fetus that was too large. One Dutch Warmblood foal was euthanized because of a combination of a ruptured inguinal hernia and bladder rupture, the other because of an acute equine herpes virus, type 1 infection.

Sample Preparation

Tarsal joints were collected within 2 h after death and stored at 4, or −18°C, the latter when further processing would occur more than 12 h after collection. If necessary, the joints were thawed in running tap water before removing all soft tissue. Articular surfaces were macroscopically inspected, photographed, and fixated in 4% buffered formaldehyde for at least a week. In order to fit in the micro-CT sample holder (diameter 7.85 cm), the distal tibias were cut transversely through the distal metaphysis about 1 cm proximal to the distal physis. The Warmblood foals' tali were cut in longitudinal direction through the middle of the talar trochlea and the two parts were scanned separately.

Micro-CT

Micro-CT imaging was performed with a μCT 80 scanner (Scanco Medical AG). Bone samples were placed in the sample holder in a consistent manner and secured with synthetic foam. Scanning was performed in air at an isotropic spatial resolution of 37 μm, with a peak voltage of 70 kV and intensity (current) of 114 μA. To reduce beam hardening effects, the scanner was equipped with an aluminium filter.

Trabecular microarchitecture was quantitatively determined in volumes of interest (VOIs) that were manually drawn and included only trabecular bone. Blood vessels present in the bone structure were not included. The VOIs comprised areas where high postnatal loading was expected. For the distal tibiae these areas were similar for foals and calves. The tibial VOI contained the trabecular bone of the dorsal 25% of the sagittal ridge (Fig. 1A,B). The average volume of this VOI was about 1,500 mm^3 (range ~800–2,100 mm^3) for the calves, 1,250 mm^3 (~900–2,000 mm^3) for the Warmblood foals, and 175 mm^3 (~100–300 mm^3) for the Shetland foals.

Species specific differences in anatomy led to the selection of different anatomical areas in the talus as "high postnatal loading" regions. As bovine tali exhibit a rather upright position, with little developed ridges, bovine talar VOIs comprised the distal part

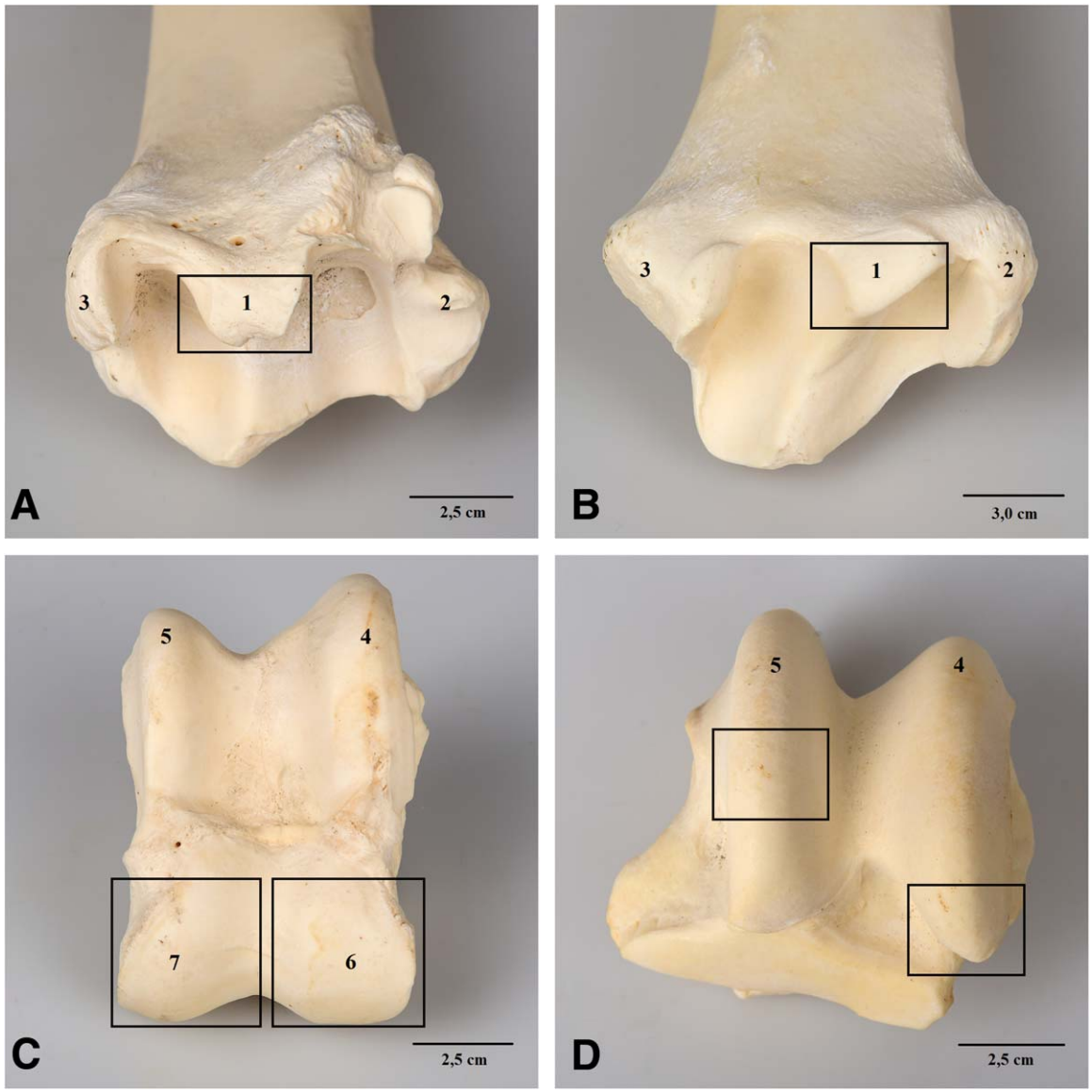

Fig. 1. Volumes of interest (VOIs) indicated with a box in samples of an (adult) distal tibia and talus. The VOI in the bovine (**A**) and equine (**B**) distal tibia consisted of the dorsal part of the sagittal ridge of the tibia. The VOI in the bovine talus (**C**) contained the medial and lateral part of the caput tali. The VOI in the equine talus (**D**) contained the distal part of the lateral and middle region of the medial talar ridge. 1: Dorsal part of the sagittal ridge of the tibia, 2: Lateral malleolus of the tibia, 3: Medial malleolus of the tibia, 4: Lateral trochlear ridge of the talus, 5: Medial trochlear ridge of the talus, 6: Lateral part of the caput tali, 7: Medial part of the caput tali. [Color figure can be viewed in the online issue, which is available at wileyonlinelibrary.com.]

of the talus (caput tali), an area that is not supported by the os malleolare (Nickel et al., 2005). The caput tali was further divided into a lateral part (average volume 1,700 mm^3, ~1,000–2,500 mm^3) and medial part (average volume 2,200 mm^3, ~1,000–3,500 mm^3, Fig. 1C), by drawing a vertical line through the middle of it.

In the horse, the trochlear ridges are prominent and slanting and the caput tali is very small (Nickel et al., 2005). Consequently, the load transmitted from the tibia has both a shear component and a component perpendicular to the ridges (Badoux, 1987), justifying the selection of the trochlear ridges as areas where high postnatal loading is expected. The lateral talar VOI consisted of the distal part of the lateral ridge (Warmblood foals: average volume 1,100 mm^3, ~800–1,500 mm^3; Shetland foals: 200 mm^3, ~150–250 mm^3; Fig. 1D). The medial talar VOI contained the middle region of the medial talar ridge (Warmblood foals: average volume 1,900 mm^3, ~1,000–3,000 mm^3; Shetland foals: 300 mm^3, ~200–500 mm^3; Fig. 1D). Both VOIs had a length of approximately 25% of the total length of the ridge and were limited by a virtual line following the deepest part of the talar trochlea.

Thresholding (i.e., distinguishing between bone and non-bone) was performed visually by comparing segmented images at different threshold levels with the original scans (representative examples of each can be seen in supporting information Figs. S1 and S2), choosing the best fit (Wolschrijn and Weijs, 2004). This procedure led to a threshold of 145 per mille of the maximum possible voxel value, corresponding to 1,222 Hounsfield units and appeared to be identical in all animals studied. This threshold is less than commonly used for trabecular bone in full-grown animals, because the bone tissue in neonatal animals is not fully mineralized and may contain cartilaginous

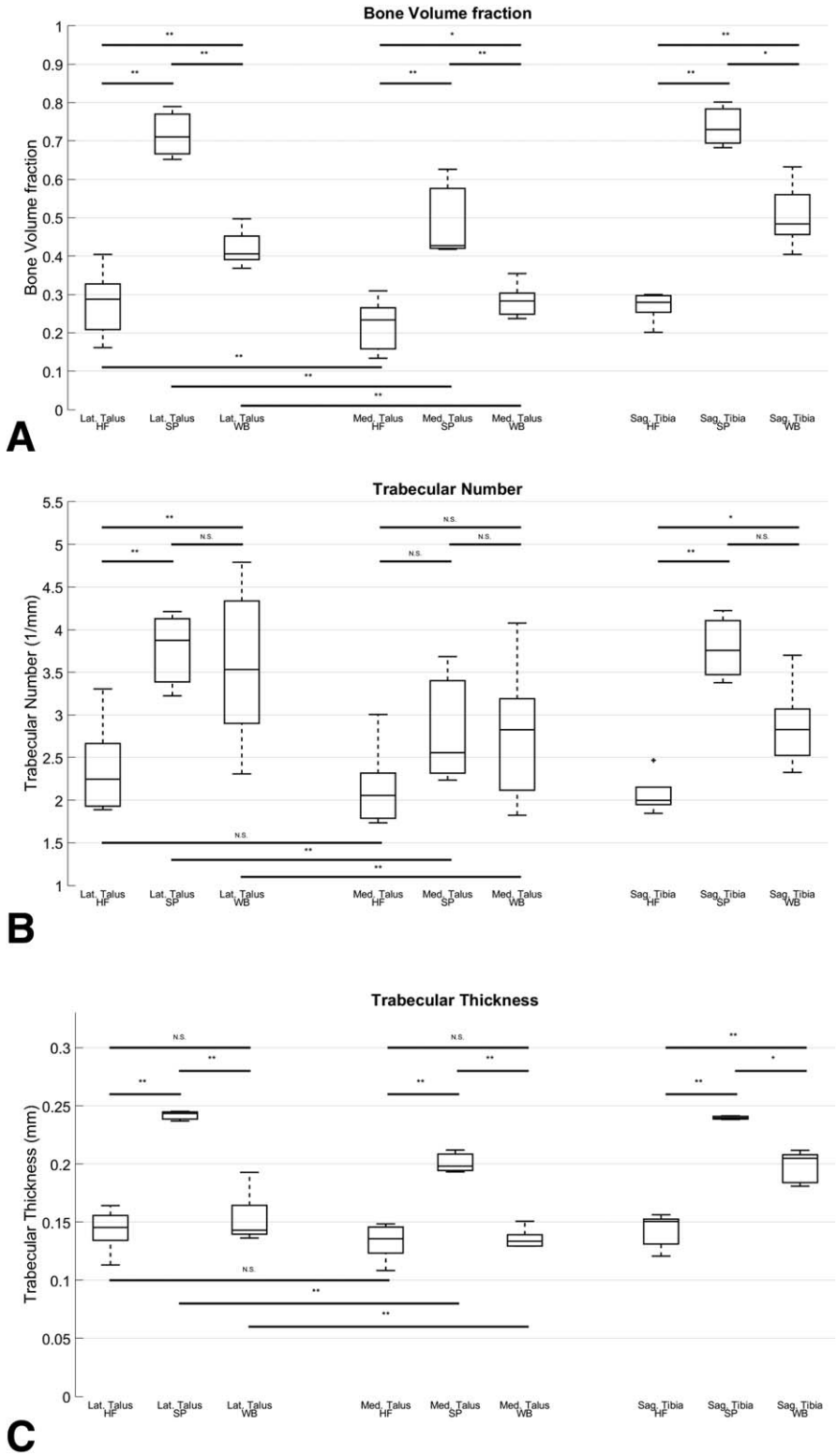

Fig. 2. Fig. 2. (A–E) Boxplots of A: Bone Volume fraction (BV/TV), B: Trabecular Number (Tb.N.), C: Trabecular Thickness (Tb.Th.), D: Trabecular Separation (Tb.Sp) and E: Directional Anisotropy (DA) calculated for the different VOIs (Lat. Talus: lateral part of the talus; Med. Talus: medial part of the talus; Sag. Tibia: sagittal ridge of the tibia) and species (HF: Holstein-Friesian calves; SP: Shetland pony foals; WB: Warmblood foals). N.S., not significant; *$0.01<P<0.05$; **$P<0.01$.

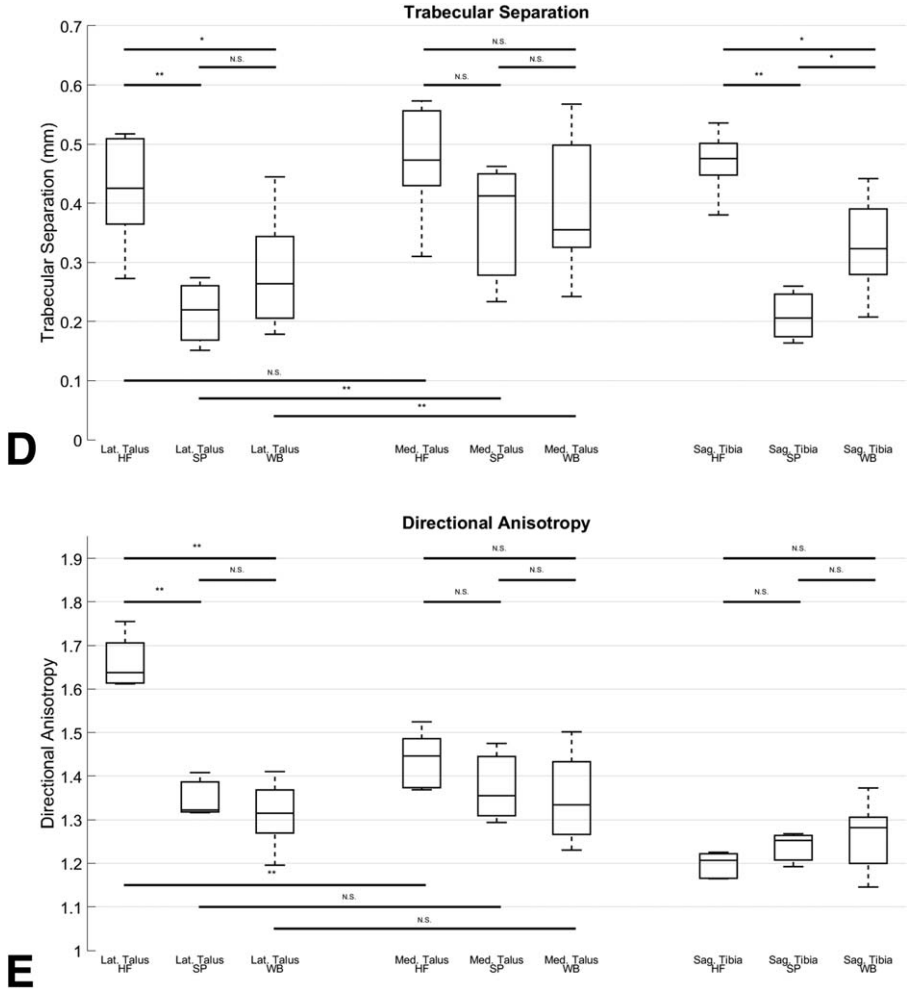

Fig. 2. (Continued)

fragments. Quantitative trabecular parameters were calculated from these segmented images with the manufacturer's software. Bone volume was calculated as the number of bone voxels divided by the total number of voxels in the VOI after segmentation. Structural parameters included trabecular number (Tb.N.), trabecular thickness (Tb.Th.), and trabecular separation (Tb.Sp.) and were calculated using a distance transformation method. The DA was based on the Mean Intercept Length fabric tensor and defined as the largest principal fabric value over the smallest one.

Statistical Analyses

Statistical analyses were performed using SPSS Statistics 22 (IBM Corporation). A paired Student's *t*-test showed no significant differences between left and right limb results for all parameters, justifying the calculation of one average value for each parameter and region studied in each animal. Trabecular parameters were log-transformed to meet normality and homoscedasticity assumptions. A linear mixed effect model, with "animal ID" added as random intercept to account for correlation between observations in the same animal, was used to check for significant differences in homologous bone regions between animal species and compare trabecular bone parameters of the lateral talar VOI with the medial talar VOI within the foals and calves. Statistical significance was set at $P \leq 0.05$ and correction for multiple comparisons was done with the False Discovery Rate method of Benjamini and Hochberg (1995).

RESULTS

Trabecular bone parameters for the VOIs are given in Figure 2. An average bone volume fraction (BV/TV) of up to 74% was found in the dorsal part of the sagittal ridge of the tibia in Shetland pony foals, whereas in Warmblood foals this was 51% and in calves 28% (Fig. 2A). The BV/TV in the lateral VOI of the talus was in the same range as in the tibia, whereas the medial VOI showed much lower values: 49% and 28% for Shetland pony and Warmblood foals, respectively, and 22% for calves. All differences in BV/TV were statistically significant.

Significantly lower trabecular numbers were found in the tibial and lateral talar VOI in calves compared to foals, whereas in the medial VOI of the talus no significant differences between the species were found (Fig. 2B).

In the Shetland pony foals, trabecular thickness was between 0.20 and 0.24 mm, which was significantly larger than in Warmblood foals (0.13–0.20 mm) and calves (0.13–0.14 mm) for all VOIs. Between Warmbloods and calves, differences were only significant in the tibia (Fig. 2C).

The highest trabecular separation values were found in the calves and differences were significantly higher compared to the foals in both the tibial and lateral talar VOIs (Fig. 2D). In the medial talar VOI, no significant differences were found. Only in the tibial VOI differences found between Warmblood and Shetland foals were significant.

The highest DA values were found in the lateral VOI of the talus of calves and were significantly different from the foals (Fig. 2E). In the tibia and medial talar VOIs, lower and not significantly different DA values were found.

When comparing trabecular architecture found in the medial talar VOI with the lateral talar VOI of the same species, BV/TV was significantly higher in the lateral talar VOI of both foals and calves. In foals, Tb.N. and Tb.Th were significantly higher, whereas Tb.Sp. was significantly lower in the lateral VOI. No difference in DA was found in the foals, whereas calves showed significantly higher DA in the lateral compared to the medial VOI of the talus.

Supporting information Figure S1 shows two-dimensional, unsegmented micro-CT transections of the left distal tibia and talus of a calf (A–C), Shetland pony foal (D–F), and Warmblood foal (G–I) showing the differences in anatomy between the animals studied. Supporting information Figure S2 contains transections of the segmented three-dimensional reconstructions of representative examples of all studied VOIs, visualizing and illustrating the described differences in trabecular bone architecture.

DISCUSSION

In order to identify possible anticipatory strategies in bone development, this study compared trabecular bone architecture at birth in the distal tibia (epiphysis of a long bone) and talus (short bone) of precocials. As it is difficult to obtain still born animals meeting the inclusion criteria, the number of animals in this study was relatively small. Nonetheless, we were able to show that foals and calves appear to have different strategies for reinforcement in the talus. In foals BV/TV is higher, whereas in calves a less dense but more anisotropic architecture is present. The DA in the calf is along a proximo-distal line through the talus, matching postnatal loading during standing and walking. As the limbs of foals and calves cannot be extended during the last part of gestation, it is tempting to hypothesize that the observed DA in the calf is not a result of the common mechanostat principle of bone development and loading (Frost and Jee, 1994; Tanck et al., 2001), but presents evidence for the existence of an anticipatory mechanism in trabecular bone growth, as has been suggested previously (Skedros et al., 2007; Cunningham and Black, 2009).

If trabecular bone in precocial neonates is indeed anticipating loading, its architecture must reflect future (postnatal) instead of past (prenatal) loading. To identify these anticipatory strategies, it is important to study areas in which significant postnatal loading is expected. In the talus noticeable anatomical differences are present, affecting the loading of this bone. In ruminants the talus is more rectangular, the trochlear ridges are aligned in the sagittal plane but are less developed; in the horse the trochlear ridges are prominent and slanting. In addition, the bovine talus is stabilized on the lateral side by the os malleolare and lateral parts of the calcaneus, whereas the equine talus is stabilized by the tight interlocking of the talar ridges in the tibial cochlea (Nickel et al., 2005). These anatomical differences have biomechanical consequences with the ruminant talus mainly perpendicularly loaded and hence experiencing compression, whereas the equine talus experiences both shear and compressive forces (Badoux, 1987).

The "volumes of interest" used in this study were chosen based on the expected loading condition immediately after birth. Defining and comparing bone regions in different species is difficult due to the species specific differences in anatomy and associated loading, which could be considered a limitation of this study. We studied the caput tali of the bovine samples as we expected to find most prominent anticipatory behavior in this region. We divided the caput tali into a lateral and medial part as it is reported that maximum pressure is found under the dorsolateral part of the hind claws in adult cattle (van der Tol et al., 2002). Loading of the equine tibia leads to tensile strain on the lateral part and compression on the medial part of the talus (Schneider et al., 1982). Strain is reported to be highest on the dorsal and lateral parts of the equine tarsal joint (Schamhardt et al., 1989; Murray et al., 2004). Accordingly, subchondral bone thickness of the os tarsi centale, positioned under the talus, was reported to be greatest on the dorsal and lateral aspects. This suggests that compressive loading is transferred from medial to lateral through the talus (Branch et al., 2005), justifying our choice for the mid region of the medial and distal part of the lateral trochlear ridges as VOI.

Average birthweight of HF calves is about 45 kg, but can easily be in excess of 60 kg (Linden et al., 2009). The calves included in this study were all above average in size and bodyweight. Warmblood foals weigh about 55–60 kg at birth (van Weeren et al., 1999; Hendriks et al., 2009). Scientific information regarding the birthweight of Shetland pony foals is difficult to obtain and limited to a paper

from the 1930s, mentioning birthweights of about 20 kg (Walton and Hammond, 1938). The bodyweight of the dams from this study are still representative for the standard sized Shetland pony nowadays, making this estimation still useful. As Shetland pony foals are much smaller at birth, VOI sizes were proportionally scaled to the size of the foal to prevent oversampling or analyzing areas not homologous in function with the Warmblood horse (Fajardo and Müller, 2001; Lazenby et al., 2011).

Bone volume fraction is a good indicator of bone strength (Kabel et al., 1999; Borah et al., 2000; Ryan et al., 2010) and it has been shown in interspecies comparisons (mainly from adult animals), that this parameter is independent of body weight (Doube et al., 2011; Barak et al., 2013; Christen et al., 2015) enabling comparison of differently sized animals. Bone volume fractions found in (Warmblood) foals were the highest, while BV/TV in the calves was much lower, although both species are comparable in birth weight and postnatal behavior. However, in the foal's talus, loading is multidirectional, as explained above, which may explain lower DA and higher BV/TV compared to the calves. Both in the calves and foals, highest BV/TV, and/or DA was observed in the lateral part, which is in line with the load distribution in the postnatal animal, providing further evidence for the anticipatory development of bone.

The BV/TV fraction in the Shetland pony was higher than in the Warmbloods. A similar result has been reported for the carpal bones, in which relative bone density was higher in ponies compared to thoroughbreds (Abdunnabi et al., 2012). This observation may be somewhat unexpected at first site, given the fact that, at least in adults, BV/TV is independent of body mass (Barak et al., 2013), but can most likely be attributed to differences in growth rate. High rates of bone growth are associated with less dense bone (Martin and Burr, 1989; Leterrier and Nys, 1992; Williams et al., 2004; Prisby et al., 2014) and growth rate in pony breeds is much lower than in horse breeds.

Other variables measured and statistically compared between groups in this study (Tb.N., Tb.Th., and Tb.Sp.) scale with negative allometry with body mass (Doube et al., 2011; Ryan and Shaw, 2013; Christen et al., 2015). Besides differences in loading described above, the lower Tb.N found in calves compared to Warmblood foals could in part be explained by their lower birth weight. However, Shetland pony foals showed the highest Tb.N. whereas their birth weight is the lowest. Just as for the BV/TV this could be caused by differences in growth rate. Furthermore, it must be emphasized that scaling factors are based on studies performed in (more) mature subjects and information about neonatal bone is lacking in literature.

In the physes of long bones, very young, newly formed bone, is reported to be anisotropic as its structure reflects the parallel columnar organization of the endochondral ossification process (Lai and Mitchell, 2005; Gosman and Ketcham, 2009). In foals ossification of the talus starts at 8 months of gestation and progresses distally and radially away from the center (Fontaine et al., 2013); for the calf this moment has not been determined yet, but it seems reasonable to assume that in this species ossification of the talus also starts in the last trimester of gestation. Therefore, it is plausible to assume that the DA observed in this study, which does not resemble the original organization, is not a primary feature of newly formed bone, but is the result of mini-modeling.

Our results, combined with previous work (Cunningham and Black, 2009; Skedros et al., 2004, 2007) show that bone (mini-)modeling can occur unrelated to loading during "special occasions," like prenatal development. Hibernation is another of such occasion as bears keep bone formation and resorption well-balanced during the hibernation period, whereas disuse would normally lead to bone resorption and osteoporosis. Through this mechanism bears preserve their bone strength to prevent problems when waking up and becoming mobile again (McGee-Lawrence et al., 2009, 2015). This situation is comparable with that of precocial animals after birth, as in both cases the skeleton must be prepared for a sudden increase in loading and this strategy saves valuable energy.

Although our data confirm anticipatory development of trabecular bone architecture to postnatal loading, which could be the result of a genetic blueprint as proposed by others (Cunningham and Black, 2009), convincing explanations for the observed differences between foals and calves are still lacking. Besides species-specific anatomy and related loading patterns, the availability of calcium could also play a role. From the literature, it is known that at equal levels of intake, horses absorb more dietary calcium from their intestine than ruminants (Schryver et al., 1983), which may help in increasing bone volume. Furthermore, gestational length in horses (11 months) is longer than in cows (9 months), giving them more time to increase their bone volume.

CONCLUSION

The results of this study illustrate that bone is a highly efficient tissue that is able to anticipate postnatal loading on a very local scale. On the level of trabecular bone, different strategies in anticipatory bone development seem to be present in the talus of calves and foals, which is likely related to anatomical differences in joint geometry and related loading patterns.

AUTHOR CONTRIBUTIONS

BMCG contributed to the concept and design of the study, acquisition, analysis, and interpretation

of the data and drafting and revision of the manuscript. CFW contributed to the concept and design of the study, data interpretation and drafting, and critical revision of the manuscript. AAM van V contributed to the acquisition, analysis, and interpretation of the data. B van R contributed to the data analysis and interpretation and critical revision of the manuscript. PR van, W contributed to the concept and design of the study, data analysis and interpretation, and critical revision of the manuscript. All authors read and approved the manuscript.

ACKNOWLEDGMENTS

The authors are grateful to the owners for giving consent and cooperating veterinary practices for their help with the collection of the tarsal joints. Furthermore they would like to thank J.C.M. Vernooij for his help with the statistical analysis.

CONFLICT OF INTEREST

The authors have no financial or personal relationship that could inappropriately influence or bias the content of this article.

LITERATURE CITED

Abdunnabi AH, Ahmed YA, Philip CJ, Davies HM. 2012. Morphometrical variations of the carpal bones in thoroughbreds and ponies. Anat Histol Embryol 41:139–148.

Badoux DM. 1987. Some biomechanical aspects of the structure of the equine tarsus. Anat Anz 164:53–61.

Barak MM, Lieberman DE, Hublin JJ. 2013. Of mice, rats and men: Trabecular bone architecture in mammals scales to body mass with negative allometry. J Struct Biol 183:123–131.

Benjamini Y, Hochberg Y. 1995. Controlling the false discovery rate: A practical and powerful approach to multiple testing. J R Stat Soc Ser B Stat Methodol 57:289–300.

Borah B, **Dufresne TE Cockman MD**, Gross GJ, Sod EW, Myers, WR, Combs KS, Higgins RE, Pierce SA, Stevens ML. 2000. Evaluation of changes in trabecular bone architecture and mechanical properties of minipig vertebrae by three-dimensional magnetic resonance microimaging and finite element modeling. J Bone Miner Res 15:1786–1797.

Branch MV, Murray RC, Dyson SJ, Goodship AE. 2005. Is there a characteristic distal tarsal subchondral bone plate thickness pattern in horses with no history of hindlimb lameness? Equine Vet J 37:450–455.

Christen P, Ito K, Ellouz R, Boutroy S, Sornay-Rendu E, Chapurlat RD, van Rietbergen B. 2014. Bone remodelling in humans is load-driven but not lazy. Nat Commun 5:4855.

Christen P, Ito K, van Rietbergen B. 2015. A potential mechanism for allometric trabecular bone scaling in terrestrial mammels. J Anat 226: 236–243.

Cunningham CA, Black SM. 2009. Anticipating bipedalism: Trabecular organization in the newborn ilium. J Anat 214: 817–829.

Doube M, Kłosowski MM, Wiktorowicz-Conroy AM, Hutchinson JR, Shefelbine SJ. 2011. Trabecular bone scales allometrically in mammals and birds. Proc Biol Sci 278:3067–3073.

Dowthwaite JN, Rosenbaum PF, Sames CA, Scerpella TA. 2014. Muscle function, dynamic loading, and femoral neck structure in pediatric females. Med Sci Sports Exerc 46:911–919.

Ducro BJ, Bovenhuis H, Back W. 2009. Heritability of foot conformation and its relationship to sports performance in a Dutch Warmblood horse population. Equine Vet J 41:139–143.

Evans HE. 1993. Miller's Anatomy of the Dog, 3rd ed. Philadelphia, PA: W.B. Saunders Company. pp 32–97.

Fajardo RJ, Müller R. 2001. Three-dimensional analysis of nonhuman primate trabecular architecture using micro-computed tomography. Am J Phys Anthropol 115:327–336.

Fontaine P, Blond L, Alexander K, Beauchamp G, Richard H, Laverty S. 2013. Computed tomography and magnetic resonance imaging in the study of joint development in the equine pelvic limb. Vet J 197:103–111.

Frost HM. 2001. From Wolff's law to the Utah paradigm: Insights about bone physiology and its clinical applications. Anat Rec 262:398–419.

Frost HM, Jee WS. 1994. Perspectives: A vital biomechanical model of the endochondral ossification mechanism. Anat Rec 240:435–446.

Gosman JH, Ketcham RA. 2009. Patterns in ontogeny of human trabecular bone from SunWatch Village in the Prehistoric Ohio Valley: General features of microarchitectural change. Am J Phys Anthropol 138:318–332.

Hendriks WK, Colenbrander B, van der Weijden GC, Stout TA. 2009. Maternal age and parity influence ultrasonographic measurements of fetal growth in Dutch Warmblood mares. Anim Reprod Sci 115:110–123.

Huiskes R, Weinans H, Grootenboer HJ, Dalstra M, Fudala B, Slooff TJ. 1987. Adaptive bone-remodeling theory applied to prosthetic-design analysis. J Biomech 20:1135–1150.

Kabel J, Odgaard A, van Rietbergen B, Huiskes R. 1999. Connectivity and the elastic properties of cancellous bone. Bone 24:115–120.

Küpfer M, Schinz HR. 1923. Beiträge zur Kenntnis der Skelettbildung bei domestizierten Säugern auf Grund röntgenlogischer Untersuchungen. Denkschriftender Schweiz Naturforsc Gesellsc 49.

Lai LP, Mitchell J. 2005. Indian hedgehog: Its roles and regulation in endochondral bone development. J Cell Biochem 15: 1163–1173.

Lazenby RA, Skinner, Kivell TL Hublin JJ. 2011. Scaling VOI size in 3D μCT studies of trabecular bone: A test of the oversampling hypothesis. Am J Phys Anthropol 144:196–203.

Leterrier C, Nys Y. 1992. Composition, cortical structure and mechanical properties of chicken tibiotarsi: Effect of growth rate. Br Poult Sci 925–939.

Linden TC, Bicalho RC, Nydam DV. 2009. Calf birth weight and its association with calf and cow survivability, disease incidence, reproductive performance, and milk production. J Dairy Sci 92:2580–2588.

MacLatchy L, Müller R. 2002. A comparison of the femoral head and neck trabecular architecture of Galago and Perodicticus using micro-computed tomography (microCT). J Hum Evol 43:89–105.

Martin RB, Burr DB. 1989. Structure, Function and Adaptation of Compact Bone. New York: Raven Press.

McGee-Lawrence ME, **Wojda SJ Barlow LN**, Drummer TD, Castillo AB, Kennedy O, Condon KW, Auger J, Black HL, Nelson OL, Robbins CT, Donahue SW. 2009. Grizzly bears (*Ursus arctos horribilis*) and black bears (*Ursus americanus*) prevent trabecular bone loss during disuse (hibernation). Bone 45:1186–1191.

McGee-Lawrence M, Buckendahl P, Carpenter C, Henriksen K, Vaughan M, Donahue S. 2015. Suppressed bone remodeling in black bears conserves energy and bone mass during hibernation. J Exp Biol 218:2067–2074.

Mittra E, Rubin C, Qin YX. 2005. Interrelationship of trabecular mechanical and microstructural properties in sheep trabecular bone. J Biomech 38:1229–1237.

Murray RC, Dyson SJ, Weekes J, Branch MV, Hladick S. 2004. Nuclear scintigraphic evaluation of the distal tarsal region in normal horses. Vet Radiol Ultrasound 45:345–351.

Nickel R, Schummer A, Seiferle E. 2005. Lehrbuch der Anatomie des Haustiere. Band I, Bewegungsapparat. Stuttgart: Parey Verlag. pp 110–128.

Pitsillides AA. 2006. Early effects of embryonic movement: 'a shot out of the Dark'. J Anat 208:417–431.

Prisby R, **Menezes T Campbell** J, Benson T, Samraj E, Pevzner I, Wideman RF Jr. 2014. Kinetic examination of femoral bone modeling in broilers. Poult Sci 93:1122–1129.

Rot I, Mardesic-Brakus S, Costain WJ, Saraga-Babic M, Kablar B. 2014. Role of skeletal muscle in mandible development. Histol Histopathol 11:1377–1394.

Ryan TM, Krovitz GE. 2006. Trabecular bone ontogeny in the human proximal femur. J Hum Evol 51:591–602.

Ryan TM, Shaw CN. 2013. Trabecular bone microstructure scales allometrically in the primate humerus and femur. Proc R Soc B 280:20130172.

Ryan WF, Lynch PB, O'Doherty JV. 2010. Survey of cull sow bone and joint integrity in the Moorepark Research Farm herd. Vet Rec 27:268–271.

Schamhardt HC, Hartman W, Lammertink JL. 1989. Forces loading the tarsal joint in the hindlimb of the horse, determined from in vivo strain measurements of the third metatarsal bone. Am J vet Res 50:728–733.

Schneider RK, Milne DW, Gabel AA, Groom JJ, Bramlage LR. 1982. Multidirectional in vivo strain analysis of the equine radius and tibia during dynamic loading with and without a cast. Am J Vet Res 43:1541–1550.

Schryver HF, Foose TJ, Williams J, Hintz HF. 1983. Calcium excretion in feces of ungulates. Comp Biochem Physiol A Comp Physiol 74:375–379.

Skedros JG, Hunt KJ, Bloebaum RD. 2004. Relationships of loading history and structural and material characteristics of bone: Development of the mule deer calcaneus. J Morphol 259:281–307. [Erratum in J Morphol (2005) 265:244-247].

Skedros JG, Sorenson SM, Hunt KJ, Holyoak JD. 2007. Ontogenetic structural and material variations in ovine calcanei: A model for interpreting bone adaptation. Anat Rec 290: 284–300.

Staines KA, Pollard AS, McGonnell IM, Farquharson C, Pitsillides AA. 2013. Cartilage to bone transitions in health and disease. J Endocrinol 219:R1–R12.

Tanck E, Homminga J, van Lenthe GH, Huiskes R. 2001. Increase in bone volume fraction precedes architectural adaptation in growing bone. Bone 28:650–654.

Torcasio A, Jähn K, Van Guyse M, Spaepen P, Tami AE, Vander Sloten J, Stoddart MJ, van Lenthe GH. 2014. Trabecular bone adaptation to low-magnitude high-frequency loading in microgravity. PLoS One 9:e93527.

Ulrich D, Hildebrand T, Van Rietbergen B, Müller R, Rüegsegger P. 1997. The quality of trabecular bone evaluated with micro-computed tomography, FEA and mechanical testing. Stud Health Technol Inform 40:97–112.

Van der Tol PP, Metz JH, Noordhuizen-Stassen EN, Back W, Braam CR, Weijs WA. 2002. The pressure distribution under the bovine claw during square standing on a flat substrate. J Dairy Sci 85:1476–1481.

van Weeren PR, Sloet v. O-O, Barneveld A. 1999. The influence of birth weight, rate of weight gain and final achieved height and sex on the development of osteochondrotic lesions in a population of genetically predisposed Warmblood foals. Equine Vet J Suppl 31:26–30.

Walton A, Hammond J. 1938. The maternal effects on growth and conformation in Shire horse-Shetland Pony crosses. Proc R Soc Lond Biol 125:311–335.

Williams B, Waddington D, Murray DH, Farquharson C. 2004. Bone strength during growth: Influence of growth rate on cortical porosity and mineralization. Calcif Tissue Int 74:236–245.

Wolff J. 1892. Das Gesetz der Transformation der Knochen. Berlin: Verlag von August Hirschwald.

Wolschrijn CF, Weijs WA. 2004. Development of the trabecular structure within the ulnar medial coronoid process of young dogs. Anat Rec A Discov Mol Cell Evol Biol 278:514–519.

Yokota H, Leong DJ, Sun HB. 2011. Mechanical loading: Bone remodeling and cartilage maintenance. Curr Osteoporos Rep 9:237–242.